



NTNU

Kunnskap for en bedre verden

DEPARTMENT OF ENGINEERING
CYBERNETICS

TTK4551 ENGINEERING CYBERNETICS,
SPECIALIZATION PROJECT

Control of a magnetic levitation system using feedback linearization

Pål Ivar Delphin Kværnø Fosmo

Supervised by

Damiano Varagnolo

Hans Alvar Engmark

January 17, 2024

Preface

This project thesis was produced during the fall semester of 2023 at the Department of Engineering Cybernetics. It is a result of the course *TTK4551 Engineering Cybernetics, Specialization Project* and serves as a preliminary thesis ahead of the master thesis in the spring of 2024. This thesis therefore marks the beginning of the last endeavour at NTNU, and provides good insight into the systems and tasks

I would like to thank Damiano Varagnolo and Hans Alvar Engmark for assigning me this fascinating and engaging task, and for including me in the future plans for the project. Their follow-up and continuous communication throughout the project has been important, and their vision for the project bodes well for the future.

I would also like to thank my fellow students Sverre Graffer and Sacit Ali Senkaya who have worked with other tasks on the same project. It has been important having sparring partners with the same knowledge of the system throughout the semester to exchange ideas with.

Pål Ivar Delphin Kværnø Fosmo

Abstract

This project thesis aims to develop a feedback linearization-based controller for a magnetic levitation system. The system consists of a circular base with embedded sensors on a printed circuit board and magnets mounted on top. The magnets are mounted in a configuration where four permanent magnets are mounted on the outer circumference of the board, with four solenoids mounted on a circumference closer to the center of the board. Above the PCB a permanent magnet will levitate in the field generated by the base. Between them an acrylic disc is mounted in order to protect the board from impacts by the levitating magnet.

The main goal is to successfully obtain and formulate a controller which can implement an advanced control method to stabilize the levitating magnet. Using a nonlinear control method called feedback linearization enables the controller to mitigate the nonlinear components of the system and from there use a control law to stabilize it, e.g. pole placement.

The system is modeled using Newton-Euler Equations of Motion together with magnet field theory, more specifically Biot-Savart's law for calculating the magnetic field and from this being able to calculate force and torque. For simulation of the system, powerful digital tools such as MATLAB and Simulink are used extensively.

The state space model of the system is modified such that it fulfills the criteria for feedback linearization. This entails extracting the input from the nonlinear function, such that the system becomes input affine. When the system fulfills the criteria and the input has been extracted, obtaining a controller is straight forward when the nonlinear components to be eliminated are identified.

Together with the feedback linearization a pole placement controller is employed to control the system to a reference signal. To evaluate the controller's performance under different circumstances a model was built in Simulink. A key area is testing how much of a limit can be put on the usage of the input before the controller stops working properly. This has to be done in order to prove the feasibility of a successful implementation on the physical system, where the solenoids have an upper limit to the current they can handle.

The resulting controller can be proved to provide convergence of the states to a reference signal. The controller therefore works as intended under the circumstances provided in the simulator, which differs somewhat from the circumstances on the physical system, where the full-state measurements are unavailable. This serves as a proof of concept for further work with this controller on the project.

In the future the work with this particular part of the project will revolve around implementing the controller on the physical system. This means that the controller formulated in this thesis will be adapted to reflect the uncontrollability of two of the states among other things. The controller will also be modified to work better with a state estimator, and will also be tested extensively with regards to noise suppression.

Sammendrag

Denne prosjektoppgaven har som mål å utvikle en tilbakekoblingslineariseringsbasert regulator for et magnetisk levitasjonssystem. Systemet består av en rund base med innebygde sensorer på et kretskort og magneter montert på toppen. Magnetene er plassert i en konfigurasjon der fire permanente magneter er montert på den ytre omkretsen av kortet, mens fire solenoider er montert på en omkrets nærmere sentrum av kortet. Over kortet vil en permanent magnet sveve i feltet som genereres av basen. Mellom dem er en disk av akrylglass montert for å beskytte kortet mot eventuelle skader fra den svevende magneten.

Hovedmålet er å utvikle en regulator som kan implementere en avansert reguleringsmetode for å stabilisere den svevende magneten. Bruk av en ikke-lineær reguleringsmetode kalt tilbakekoblingslinearisering fører til at regulatoren kan dempe de ikke-lineære komponentene i systemet. Deretter kan en lineær reguleringsmetode brukes for å stabilisere det, for eksempel polplassering.

Systemet modelleres ved bruk av Newton-Eulers bevegelsesligninger sammen med magnetfeltteori. Mer spesifikt brukes Biot-Savarts lov for å beregne det magnetiske feltet og derfra kan kraft og dreiemoment beregnes. For simulering av systemet brukes digitale verktøy som MATLAB og Simulink.

Tilstandsrommet til systemet modifiseres slik at det oppfyller kriteriene for tilbakekoblingslinearisering. Dette innebærer å skille pådraget fra den ikke-lineære funksjonen, slik at systemet blir pådragsaffint. Når systemet oppfyller kriteriene og pådraget er utskilt, er det enklere å formulere en reguleringslov, gitt at de ikke-lineære komponentene som skal elimineres kan identifiseres.

Sammen med tilbakekoblingslinearisering brukes en polplasseringsregulator for å styre systemet mot et referansesignal. For å evaluere regulatorens ytelse under forskjellige omstendigheter ble det laget en modell i Simulink. Et viktig oppdrag er å teste hvor mye begrensning som kan pålegges bruken av pådraget før regulatoren slutter å fungere. Dette må gjøres for å bevise gjennomførbarheten av en vellykket implementering på det fysiske systemet, der solenoidene har en øvre grense for strømmen de kan dra.

Den resulterende regulatoren kan vises å gi konvergens av tilstandene til et referansesignal. Regulatoren fungerer derfor som tiltenkt under forholdene som er gitt i simulatoren, noe som skiller seg noe fra forholdene på det fysiske systemet der fullstendige tilstandsmålinger er utilgjengelige. Dette fungerer som en konseptbevis for videre arbeid med denne regulatoren.

I fremtiden vil arbeidet med denne delen av prosjektet dreie seg om å implementere regulatoren på det fysiske systemet. Dette betyr at regulatoren formulert i denne avhandlingen må tilpasses for å gjenspeile blant annet ukontrollerbarheten av to av tilstandene. Regulatoren vil også bli endret slik at den vil fungere bedre med en tilstandsestimator og vil også bli testet grundig med hensyn til eventuell støysuppresjon.

Table of Contents

Preface	i
Abstract	ii
Sammendrag	iii
List of Figures	vi
1 Introduction	1
1.1 Structure of the report	1
2 Theory	3
2.1 Magnet field theory	3
2.1.1 Biot-Savart's law	3
2.1.2 Forces and torque	4
2.2 Nonlinear control	4
2.2.1 Feedback linearization	4
2.3 Mathematical tools	5
2.3.1 Distributive property of the cross product	5
2.3.2 Digital tools	5
3 System introduction	7
3.1 System description	7
3.2 System formulation	7
4 Feedback linearization	10
4.1 Input-State Linearization	10
4.2 Decomposition	11
4.2.1 Modification of magnetic field formula	11
4.2.2 Making the system input affine	11
4.2.3 Splitting the input vector	12
4.3 Controller	13
4.3.1 Tackling the matrix inverse	14
4.4 Implementation for simulation	14
5 Results	16

5.1	Controller	16
5.2	Simulation	16
5.2.1	Validation	16
5.2.2	Controller simulations	18
5.2.3	Regions of convergence	23
6	Discussion	24
6.1	Choice of controller	24
6.2	Matrix inverse	24
6.3	Regions of convergence	24
6.3.1	Stability	25
6.4	Limitation of the input	25
6.5	System identification	26
7	Further work	27
7.1	Implementation	27
7.2	Stability	27
7.3	Other control approaches	27
8	Conclusion	28
	References	29

List of Figures

1	Picture of the magnetic levitation system	7
2	Implementation in Simulink for simulations	15
3	Simulation of the original system	17
4	Simulation of the fully decomposed system (4.2.3)	17
5	Deviation between the original and the decomposed system	18
6	Simulations of the system with pure pole placement	19
7	Simulation of the controlled system with uninhibited control inputs .	19
8	Simulation of the controlled system with limited control inputs	20
9	Simulation of the controlled system with limited control inputs	20
10	Simulation of the controlled system with severely limited control inputs	21
11	Simulation of the controlled system with loosened control input limits	22
12	Simulation of the controller with step in reference without (a) and with (b) restrictions on input	22
13	Approximations of the regions of convergence for two different values of the input limit	23
14	Example of optimal testing	25

1 Introduction

The field of magnetic levitation is evergrowing and extends into many different domains and applications. Among the most notable examples being high-speed trains and even elevators. Magnetism is not a new concept, and was already known by ancient peoples through the lodestone, which is a magnetized piece of iron ore. It wasn't before the 1800s the link between electric current and magnetism was discovered, and it laid the foundations for the electromagnet. (Coey, 2010)

The magnetic levitation system (from now on called *maglev*) is developed with a clear goal of being an interactive educational tool. The system can be used to learn basic electronics and cybernetics concepts, and can double as a lab that can be successfully carried out at home. The system aims to stabilize a levitating magnet above a platform where several permanent magnets and solenoids are mounted in some configuration. Through active use of the solenoids the magnetic field can be altered to allow for stable levitation.

The task of controlling a maglev system requires precise and efficient control mechanisms, and even then it is not guaranteed that the system can be stabilized. Due to the fact that control of this system requires manipulation of magnetic fields, the system is a highly nonlinear one, and successfully controlling it will most likely include usage of an advanced control method.

The purpose of this report is to describe a feedback linearizing controller that mitigates the effects of the nonlinearities. Through a comprehensive design process with testing for analysis purposes, the controllers performance will be evaluated under different circumstances. Among the most important aspects is testing the controller in circumstances as identical to the physical system as possible. In this report the main focus is put on limiting the use of the input such that the physical limitations of the solenoids are respected whilst keeping the controller functional.

1.1 Structure of the report

This report is structured in the following way to provide insight into the process of controller development, the necessary prior knowledge and presentation and discussion of the resulting simulations.

1. The first chapter contains an introduction to the subject and a presentation of the project at hand. The project as a whole is motivated and as is the controller development.
2. The theory chapter introduces the necessary theorems and knowledge needed to fully understand the nonlinearities of the system. In addition to this, some information about the mathematical tools used are also provided together with basic nonlinear control theory related to the system.
3. The third chapter presents the physical system. Here both the physical construction of the maglev is described, as well as the formulation of the system's

dynamics.

4. This chapter is the most encompassing one and delves into the development process of the controller. The system formulation is broken down in order to make the system input affine, and from this a feedback linearizing controller is retrieved in line with the theory already presented.
5. Here the resulting controller formulation is presented, alongside simulations to determine the controllers performance with different limits put on the inputs.
6. In this chapter, the results and the choices made throughout the project are discussed and justified.
7. This chapter covers the road ahead in the project with regards to the controller. This more or less lays down guidelines for the further development and implementation of the controller on the physical system, both with regards to adaptation of the controller and tests to be conducted afterwards.
8. This chapter concludes the report with a short conclusion based on the results.

2 Theory

This section will delve into the theoretical aspects of the system and the concepts needed for the development of a controller for the maglev system.

2.1 Magnet field theory

One of the main aspects of this project is working with magnetic fields, and altering them to allow for the levitation of a free magnet. Some general knowledge about these fields is therefore needed to understand the dynamics of the system.

2.1.1 Biot-Savart's law

Biot-Savart's law is central for the calculation and description of the magnetic field generated by the solenoids. The law provides an equation relating the generated magnetic field to a constant electric current. This relationship is given by

$$\mathbf{B}(\mathbf{r}) = \frac{\mu_0}{4\pi} \int_C \frac{I d\boldsymbol{\ell} \times \mathbf{r}'}{|\mathbf{r}'|^3} \quad (1)$$

where \mathbf{r} denotes the position in 3D-space and I the current in the wire. μ_0 is the permeability of air, $d\boldsymbol{\ell}$ is a vector along the wire C while \mathbf{r}' is the displacement vector from the wire element to the point in which the field is calculated. (Grant, 1990)

In this system the solenoids are approximated as single thin wire loops in order to reduce computational times. The law's application in this system is therefore akin to the one described in the paper González and Cárdenas, 2021. The simplification reads:

$$\mathbf{B}(\phi, \rho, z) = \begin{bmatrix} \phi \\ -\frac{z}{\rho} ck \left[K(k^2) - \frac{\rho^2 + R^2 + z^2}{(\rho - R)^2 + z^2} E(k^2) \right] \\ ck \left[K(k^2) - \frac{\rho^2 - R^2 + z^2}{(\rho - R)^2 + z^2} E(k^2) \right] \end{bmatrix} \quad (2)$$

$$k^2 = \frac{4R\rho}{(R + \rho)^2 + z^2}$$
$$c = \frac{\mu_0}{4\pi\sqrt{R\rho}} NI$$

Where $K(k^2)$ and $E(k^2)$ denote the complete elliptical integrals of the first and second kind. The polar coordinates (ϕ, ρ, z) represent the distance vector from the point in space to the center point of the solenoid.

2.1.2 Forces and torque

The system's translation and rotation are modelled using Newton-Euler Equations of Motion. This means that the calculations of the magnetic fields must be translated into forces and torques exerted on the levitating magnet. Expressions for the force and torque acting on a permanent magnet of zero size in a uniform magnetic field can be written as:

$$\mathbf{F} = \nabla \left(\frac{\mathbf{J}}{\mu_0} \cdot \mathbf{B} \right) \quad (3)$$

$$\boldsymbol{\tau} = \frac{\mathbf{J}}{\mu_0} \times \mathbf{B} \quad (4)$$

where \mathbf{J} denotes the magnetic polarization of the magnet. (Sadiku, 2001)

By integrating this formula over a volume, the force and torque on an arbitrary permanent magnet can be calculated. Using the *equivalent magnetization approach* for the models of the permanent magnets, the magnetization surface current \mathbf{K} can be expressed as (Ravaud et al., 2010)

$$\mathbf{K} = \frac{\mathbf{J} \times \mathbf{n}}{\mu_0} \quad (5)$$

which allows for the forces and torques to be accurately calculated by the surface integrals over the surface \mathbf{S} of the magnets

$$\mathbf{F} = \int_{\mathbf{S}} \mathbf{K}(\alpha, \beta, \gamma) \times \mathbf{B}_{Base}(x, y, z) dS \quad (6)$$

$$\boldsymbol{\tau} = \int_{\mathbf{S}} \frac{1}{\mu_0} \mathbf{J}(\alpha, \beta, \gamma) \times \mathbf{B}_{Base}(x, y, z) dS \quad (7)$$

2.2 Nonlinear control

Systems with inherent nonlinear components does not adhere to the traditional rules laid out by linear system theory, such as *the superposition principle*. In addition to this, powerful mathematical tools such as the *Laplace* and *Fourier* transforms do not apply to this class of systems, rendering a wide range of analytical solutions for linear systems obsolete. (Slotine and Li, 1991) Linearization can be a powerful tool, but it cannot guarantee stability and convergence in cases where the states diverge too much from the operating point. (Khalil, 2002)

This means that in order to control a nonlinear system, other routes must be taken to design a controller able to deliver the stability desired.

2.2.1 Feedback linearization

The concept of controlling a nonlinear system becomes much easier if it can be likened to a linear system. Feedback linearization is a powerful tool that can achieve

this. The main idea behind this approach is to cancel the nonlinearities and impose a linear structure on the system through use of the input.

Generally, designing an input u that can directly cancel all nonlinearities in a system might prove difficult in many cases. If a system can be presented in a general semi-linear form as

$$\dot{\mathbf{x}} = A\mathbf{x} + B\gamma(u - \alpha(\mathbf{x})) \quad (8)$$

from which u can be used directly to transform the system to a linear controllable form for some domain \mathcal{D} .

This direct cancellation does have some prerequisites

1. γ must be nonsingular for every $x \in \mathcal{D}$
2. The control input u and the nonlinear term must appear together as a sum $u + \alpha(\mathbf{x})$,

The general input then takes the form

$$u = \alpha(\mathbf{x}) + \beta(\mathbf{x})v \quad (9)$$

where $\beta(\mathbf{x}) = \gamma^{-1}$ and v denotes the desired input or linear control law. (Khalil, 2002)

2.3 Mathematical tools

A wide range of mathematical tools are needed in order to properly model the system, and to successfully develop a feedback linearization controller.

2.3.1 Distributive property of the cross product

When breaking down the system, a part of the nonlinear component consists of a cross product. A fundamental property of distributivity of the cross product is helpful in this case (Lipschutz, Spiegel, and Spellman, 2009, p. 22)

$$A \times (B + C) = A \times B + A \times C \quad (10)$$

2.3.2 Digital tools

When developing the controller, extensive testing of the system is needed in order to assess the performance of the controller together with the impact it has on the dynamics. *Simulink* is a powerful modelling tool included in *MATLAB*, in which systems can be built by block diagrams and simulated over a period of time. This

both allows for an intuitive representation of the system, whilst its modular nature makes it easy to make modifications on the system.

The functions calculating the fields, forces and generating the dynamics are all written using MATLAB. For the force and torque calculations the MATLAB function *trapz* is utilized, which numerically integrates an array using the trapezoidal method. (The MathWorks, n.d.(b))

For the controller design a central concept is the usage of *mldivide* for the calculation of the inputs. This allows the code to solve a linear problem $Ax = b$ even when the matrix A is non-square using a QR solver, which is a decompositional method of solving a linear problem. (The MathWorks, n.d.(a))

3 System introduction

This section will introduce the maglev system through description of the plant, as well as establish the system's mathematical formulation as a state space.

3.1 System description

The magnetic levitation system consists of a circular PCB with four mounted stacks of neodymium magnets equally spaced on the circumference. On the inner circumference four solenoids are mounted and soldered on in the same manner. The system is driven by a *Teensy* microcontroller mounted on the pins on the underside of the PCB. Resting above the hardware is an acrylic disc which serves to protect the PCB from possible damage from the levitating magnet, which levitates above the acrylic disc.

On the PCB various other components are mounted, the most important and relevant ones being the hall-effect sensors which offer measurements of the magnetic fields. These will serve as the main measurement devices, and measures the magnetic fields in x-, y- and z-direction respectively.

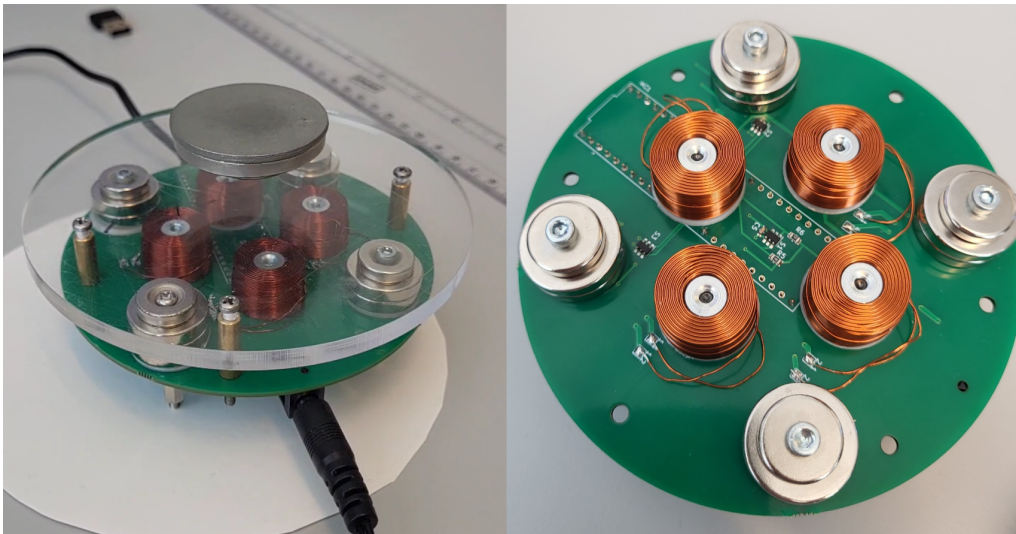


Figure 1: Picture of the magnetic levitation system

Figure 1 shows the full system as described above, and for which a controller will be developed.

3.2 System formulation

The formulation of the system dynamics are detailed in Engmark and Hoang, 2023. Using *Newton-Euler Equations of Motion* the system can be modeled for simulation. The mathematical formulation of the system and its dynamics can then be expressed

in a state space with state vector

$$\mathbf{x} = [x \ y \ z \ \alpha \ \beta \ \gamma \ \dot{x} \ \dot{y} \ \dot{z} \ \dot{\alpha} \ \dot{\beta} \ \dot{\gamma}]^T$$

Which yields

$$\dot{\mathbf{x}} = \mathbf{A}\mathbf{x} + \mathbf{B}f(\mathbf{x}, \mathbf{u}) \quad (11)$$

where

$$\begin{aligned} \mathbf{A} &= \begin{bmatrix} \mathbf{0}_6 & \mathbf{I}_6 \\ \mathbf{0}_6 & \mathbf{0}_6 \end{bmatrix} \\ \mathbf{B} &= \begin{bmatrix} \mathbf{0}_6 \\ \mathbf{I}_6 \end{bmatrix} \end{aligned} \quad (12)$$

and the nonlinear term

$$f(\mathbf{x}, \mathbf{u}) = \begin{bmatrix} m\mathbf{I}_3 & \mathbf{0}_3 \\ \mathbf{0}_3 & \mathcal{I} \end{bmatrix}^{-1} \left(\begin{bmatrix} \mathbf{F}(\mathbf{x}, \mathbf{u}) \\ \boldsymbol{\tau}(\mathbf{x}, \mathbf{u}) \end{bmatrix} - \begin{bmatrix} \mathbf{F}_g \\ \boldsymbol{\omega} \times \mathcal{I}\boldsymbol{\omega} \end{bmatrix} \right) \quad (13)$$

where force \mathbf{F} and torque \mathbf{T} are the resulting cross products of the magnetic field and the magnetization surface current vector \mathbf{K} and the magnetic polarization vector \mathbf{J} respectively. (sec. 2.1.2)

To limit computational complexity these calculations can be approximated as a summation over n partitions of the magnet

$$\mathbf{F} = \frac{2\pi Rl}{n} \sum_{i=1}^n \mathbf{K}(\alpha, \beta, \gamma) \times \mathbf{B}_{\text{base}}(x_i, y_i, z_i) \quad (14a)$$

$$\boldsymbol{\tau} = \frac{2\pi Rl}{n\mu_0} \sum_{i=1}^n \mathbf{J}(\alpha, \beta, \gamma) \times \mathbf{B}_{\text{base}}(x_i, y_i, z_i) \quad (14b)$$

\mathbf{B}_{base} represents the magnetic field present in the point (x, y, z) as produced by the n_m permanent magnets and the n_s solenoids with center points in (x_i, y_i, z_i) in the maglev-base, and is defined as

$$\mathbf{B}_{\text{base}}(x, y, z) := \sum_{i=1}^{n_s+n_m} \mathbf{B}(x - x_i, y - y_i, z - z_i) \quad (15)$$

$$\mathbf{B}(x, y, z) = \begin{bmatrix} B_\rho \cos B_\phi \\ B_\rho \sin B_\phi \\ B_z \end{bmatrix} \quad (16)$$

The total magnetic field from the base is calculated using the formula for magnetic force generated by a thin wire loop in polar coordinates (sec. 2.1.1)

$$\mathbf{B}(\phi, \rho, z) = \begin{bmatrix} \phi \\ -\frac{z}{\rho}ck \left[K(k^2) - \frac{\rho^2+R^2+z^2}{(\rho-R)^2+z^2} E(k^2) \right] \\ ck \left[K(k^2) - \frac{\rho^2-R^2+z^2}{(\rho-R)^2+z^2} E(k^2) \right] \end{bmatrix} \quad (17)$$

where

$$k^2 = \frac{4R\rho}{(R + \rho)^2 + z^2}$$
$$c = \frac{\mu_0}{4\pi\sqrt{R\rho}}NI$$

4 Feedback linearization

In a bid to control the maglev system, countless methods are available for pursuit, most of them classified as advanced. Control of magnetic levitation systems have mostly been limited to systems with magnets levitating *beneath* the actuating electromagnets. Drawing inspiration from Uswarman, Cahyadi, and Wahyunggoro, 2013, the goal of controlling the maglev system will be achieved through *feedback linearization* with a pole placement controller.

In order to facilitate a feedback linearization of the system at hand, some reformulations must be done to convert the system into a more general form from which a controller can be found. This is done both to develop the controller itself, but also to prove that the system is feedback linearizable.

4.1 Input-State Linearization

Generally, when feedback linearizing a system, one wants to formulate it in a way such that all nonlinearities are eliminable just by the input alone. That is, propose a transformation $\mathbf{z} = \mathbf{z}(\mathbf{x})$ that transforms the system into

$$\dot{\mathbf{z}} = A'\mathbf{z} + B'\mathbf{v}$$

where

$$A' = \begin{bmatrix} 0 & 1 & 0 & \dots & 0 \\ 0 & 0 & 1 & \dots & 0 \\ \vdots & \dots & \dots & 1 & \vdots \\ 0 & 0 & 0 & 0 & 0 \end{bmatrix}, B' = \begin{bmatrix} 0 \\ 0 \\ \vdots \\ 1 \end{bmatrix}$$

and \mathbf{v} denotes the new input in which the linear control law can be implemented. This approach is called *Input-State Linearization*. (Slotine and Li, 1991)

In the case of this system, it is evident that by dividing the original state vector into two vectors

$$z_1 = \begin{bmatrix} x \\ y \\ z \\ \alpha \\ \beta \\ \gamma \end{bmatrix}, z_2 = \begin{bmatrix} \dot{x} \\ \dot{y} \\ \dot{z} \\ \dot{\alpha} \\ \dot{\beta} \\ \dot{\gamma} \end{bmatrix}$$

the system can be represented in such a way that all nonlinearities occur in the same state vector, namely z_2 . This is also trivially available from the original form of the system, in which the matrices A and B already take the form of A' and B' . From this it is concluded that the system is feedback linearizable.

4.2 Decomposition

In the model described in section 3.2 the input is nested inside the nonlinear function $f(\mathbf{x}, \mathbf{u})$. This means that a feedback linearizing controller cannot easily be obtained from the equations themselves. Recall from section 2.2.1 that the desired structure of the system is

$$\dot{\mathbf{x}} = A\mathbf{x} + B\gamma(\mathbf{x})[\mathbf{u} - \alpha(\mathbf{x})]$$

in which the input is linear, or *affine*. (Slotine and Li, 1991) The first challenge is the decomposition of the nonlinear function $f(\mathbf{x}, \mathbf{u})$ to separate the input from the nonlinearities. The main objective is therefore to extract the input signal \mathbf{u} from the nonlinear function. Recall that the input of the system is the current running through the solenoids, and directly impacts the magnetic field used to calculate the force and torque acting on the levitating magnet through (14a) and (14b) linearly.

4.2.1 Modification of magnetic field formula

It becomes clear that the main obstacle lies within the two equations for force and torque respectively. The first step is therefore to retrieve the current \mathbf{I} , which is a linear term, from the calculation of each magnet's magnetic field $\mathbf{B}(\phi, \rho, z)$.

From (17), the polar coordinates can be converted to cartesian coordinates by (16), and the current I can be separated such that

$$\mathbf{B}(x, y, z) = \begin{bmatrix} -\frac{z}{\rho}c^*k[K(k^2) - \frac{\rho^2+R^2+z^2}{(\rho-R)^2+z^2}E(K^2)]\cos(\phi) \\ -\frac{z}{\rho}c^*k[K(k^2) - \frac{\rho^2+R^2+z^2}{(\rho-R)^2+z^2}E(K^2)]\sin(\phi) \\ c^*k[K(k^2) - \frac{\rho^2+R^2+z^2}{(\rho-R)^2+z^2}E(K^2)] \end{bmatrix} I \quad (18)$$

$$c^* = \frac{\mu_0}{2\pi\sqrt{R\rho}}N$$

with k unaltered. With the current isolated from the magnetic field dynamics as a linear term, the next step is to implement the same change in the $\mathbf{F}(\mathbf{x}, \mathbf{u})$ and $\boldsymbol{\tau}(\mathbf{x}, \mathbf{u})$ formulas.

4.2.2 Making the system input affine

These formulas consist of cross products between \mathbf{K} and \mathbf{J} and the magnetic field vector respectively. This means that in order to separate the current \mathbf{I} from the entire function, these cross products must be dissected further.

A vital tool for this dissection is using one of the main properties of the cross product. (sec. 2.3.1)

The distributive property of the cross product applied to $\mathbf{F}(\mathbf{x}, \mathbf{u})$ yields

$$\mathbf{F}(\mathbf{x}, \mathbf{u}) = \frac{2\pi Rl}{n} \underbrace{\left[\sum_{i=1}^n \mathbf{K}(\alpha, \beta, \gamma) \times \mathbf{B}_1 \quad \dots \quad \sum_{i=1}^n \mathbf{K}(\alpha, \beta, \gamma) \times \mathbf{B}_{n_m+n_s} \right]}_{3 \times (n_m+n_s)} \underbrace{\mathbf{I}}_{(n_m+n_s) \times 1}$$

The same reformulation can be done to $\boldsymbol{\tau}(\mathbf{x}, \mathbf{u})$ in order to fully separate the cross products from the input. After separating the input from both components of the nonlinear function, the system can be written as

$$\dot{\mathbf{x}} = \mathbf{A}\mathbf{x} + \mathbf{B}g(\mathbf{x})^{-1}(h(\mathbf{x})\mathbf{I} - p(\mathbf{x})) \quad (19)$$

where

$$\begin{aligned} g(\mathbf{x}) &= \begin{bmatrix} m\mathbf{I}_3 & \mathbf{0}_3 \\ \mathbf{0}_3 & \mathcal{I} \end{bmatrix} \\ h(\mathbf{x}) &= \begin{bmatrix} \sum_{i=1}^n \mathbf{K}(\alpha, \beta, \gamma) \times \mathbf{B}_1 & \dots & \sum_{i=1}^n \mathbf{K}(\alpha, \beta, \gamma) \times \mathbf{B}_{n_m+n_s} \\ \sum_{i=1}^n \mathbf{J}(\alpha, \beta, \gamma) \times \mathbf{B}_1 & \dots & \sum_{i=1}^n \mathbf{J}(\alpha, \beta, \gamma) \times \mathbf{B}_{n_m+n_s} \end{bmatrix} \\ p(\mathbf{x}) &= \begin{bmatrix} \mathbf{F}_g \\ \boldsymbol{\omega} \times \mathcal{I}\boldsymbol{\omega} \end{bmatrix} \end{aligned}$$

Generally, the system now has a form with which a feedback linearization normally can be implemented through the input.

4.2.3 Splitting the input vector

Up until now the vector \mathbf{I} has been referred to as the vector of inputs, which is not entirely accurate. This is a result of how the magnetic fields are calculated, where the permanent magnets are modelled in the same way as the solenoids, only with a constant corresponding current. This means that only some elements in the vector \mathbf{I} can be altered, further causing the formulation in (19) to be insufficient when trying to deduce a feedback linearization controller for the system.

To remedy this, another decomposition of the system must be done in order to separate the elements of \mathbf{I} which can be altered from the ones that cannot. In other words, to separate the real input u from the constant corresponding currents of the permanent magnets.

To achieve this, the vector of inputs \mathbf{I} is divided into a constant part and a variable part.

$$\mathbf{I} = \begin{bmatrix} \mathbf{I}_M \\ \mathbf{I}_S \end{bmatrix}$$

with the subscripts M and S denoting permanent magnet and solenoid respectively.

This also requires the matrix $h(\mathbf{x})$ to be divided into corresponding parts for the permanent magnets and the solenoids, $h_M(\mathbf{x})$ and $h_S(\mathbf{x})$ respectively. This yields

the following system formulation.

$$\dot{\mathbf{x}} = A\mathbf{x} + Bg(\mathbf{x})^{-1}(h_S(\mathbf{x})\mathbf{I}_S + h_M(\mathbf{x})\mathbf{I}_M - p(\mathbf{x})) \quad (20)$$

where

$$h_M(\mathbf{x}) = \begin{bmatrix} \sum_{i=1}^n \mathbf{K}(\alpha, \beta, \gamma) \times \mathbf{B}_1 & \dots & \sum_{i=1}^n \mathbf{K}(\alpha, \beta, \gamma) \times \mathbf{B}_{n_m} \\ \sum_{i=1}^n \mathbf{J}(\alpha, \beta, \gamma) \times \mathbf{B}_1 & \dots & \sum_{i=1}^n \mathbf{J}(\alpha, \beta, \gamma) \times \mathbf{B}_{n_m} \end{bmatrix}$$

$$h_S(\mathbf{x}) = \begin{bmatrix} \sum_{i=1}^n \mathbf{K}(\alpha, \beta, \gamma) \times \mathbf{B}_1 & \dots & \sum_{i=1}^n \mathbf{K}(\alpha, \beta, \gamma) \times \mathbf{B}_{n_s} \\ \sum_{i=1}^n \mathbf{J}(\alpha, \beta, \gamma) \times \mathbf{B}_1 & \dots & \sum_{i=1}^n \mathbf{J}(\alpha, \beta, \gamma) \times \mathbf{B}_{n_s} \end{bmatrix}$$

and \mathbf{I}_S becomes the real input u .

4.3 Controller

With the system in the decomposed form from (20) the task of finding a controller to eliminate the nonlinearities becomes easier. Furthermore, this allows for the theory described in section 2.2.1 to be directly applied to the system. In the case of the maglev system, the following definitions can be made in order to visualize the system in the desired form:

$$\gamma(\mathbf{x}) = g(\mathbf{x})^{-1}$$

$$\alpha(\mathbf{x}) = p(\mathbf{x}) - h_M(\mathbf{x})\mathbf{I}_M$$

which yields

$$\dot{\mathbf{x}} = A\mathbf{x} + B\gamma(\mathbf{x})[h_S(\mathbf{x})\mathbf{I}_S - \alpha(\mathbf{x})] \quad (21)$$

where \mathbf{I}_S denotes the real input u .

At this point, the procedure of picking a fitting control law would normally be quite trivial, using u as it appears in section 2.2.1. In this case the presence of $h_S(\mathbf{x})$ complicates matters in the sense that it introduces another variable for which the existence and uniqueness must be known for all values within the controlled domain. For $h_S(\mathbf{x})$, which contains the force and torque components for the magnetic field from the solenoids, this isn't necessarily a trivial task.

From this it generally follows that the matrix $h_S(\mathbf{x})$ must be invertible in order to find a solution for the input \mathbf{I}_S when the desired form of the controller is

$$u = \alpha(\mathbf{x}) + \beta(\mathbf{x})v$$

$$\downarrow$$

$$\mathbf{I}_S = h_S(\mathbf{x})^{-1}(\alpha(\mathbf{x}) - \gamma(\mathbf{x})^{-1}v) \quad (22)$$

In addition to the feedback linearization-aspect of the controller, a basic pole placement controller is employed as the primary method of controlling the system with

stable poles in the left-half plane for the closed-loop system. This is implemented by adding the gain matrix K multiplied by the state vector, giving the full controller the form

$$\mathbf{I}_S = h_S(\mathbf{x})^{-1}(\alpha(\mathbf{x}) - \gamma(\mathbf{x})^{-1}K\mathbf{x}) \quad (23)$$

where the gain matrix K is generated using MATLAB's *place()* for the poles

$$[-100 \quad -100 \quad -100 \quad -120 \quad -300 \quad -320 \quad -210 \quad -120 \quad -170 \quad -230 \quad -90 \quad -140]$$

4.3.1 Tackling the matrix inverse

Due to the complexity of the magnetic fields and the forces generated by them, it is hard to guarantee that the inverse of $h_S(\mathbf{x})$ exists and is unique. This combined with the fact that it is not square means that other methods must be employed in order to formulate its inverse. Numerical methods available in MATLAB can be used to remedy this, that is solving a set of linear equations in order to find \mathbf{I}_S . MATLAB's *mldivide* (sec. 2.3.2) does exactly this, basically transforming the controller to the form

$$h_S(\mathbf{x})\mathbf{I}_S = \alpha(\mathbf{x}) - \gamma(\mathbf{x})^{-1}K\mathbf{x}$$

Closing the loop with the calculated \mathbf{I}_S will in theory lead to a system formulated as

$$\dot{\mathbf{x}} = (A - BK)\mathbf{x} \quad (24)$$

in which $(A - BK)$ is Hurwitz, which yields a stable system.

4.4 Implementation for simulation

After retrieving the controller on the form given above, an implementation can be made using MATLAB and Simulink. All variables and parameters are stored in code for MATLAB through *.m*-files that can be accessed by Simulink, where the system can be built using block diagrams. This provides a nice modularity for the system, as well as intuitively visualizing the different parts and how they interact with each other.

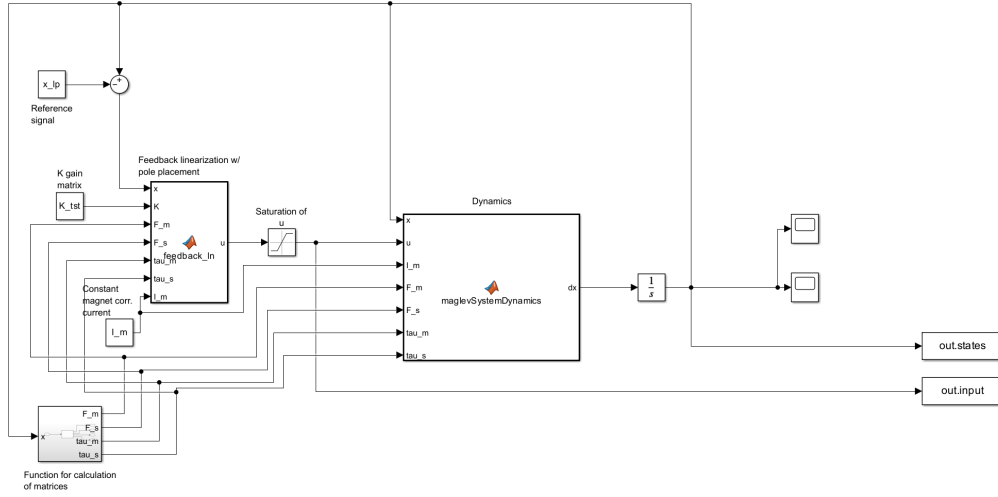


Figure 2: Implementation in Simulink for simulations

The figure above showcases the setup in Simulink used for simulations for the full state-feedback linearized controller. The controller is implemented in its separate block, as is both the dynamics and the calculations of the force and torque matrices. The Simulink block diagram is connected to the MATLAB workspace using *To Workspace* blocks to save data from simulation for plotting and further analysis in MATLAB.

Using code developed in order to facilitate simulations with this setup, plots for both the isolated performances of the controller and the regions of convergence can be produced. The code used for simulation of the model and all the functions are available through a *GitHub*-repository.¹

¹https://github.com/Paalfosmo/MAGLEV_project_control

5 Results

In this section the developed controller will be presented together with the tests carried out in Simulink. The plots from the validation tests done for the decomposition of the system in addition to approximations of the regions of convergence for the controller also be presented here.

5.1 Controller

By using feedback linearization on the full state space of the system model, the following control law was found to suppress the nonlinearities in the system and implement a pole placement controller:

$$h_s(\mathbf{x})u = p(\mathbf{x}) - h_M(\mathbf{x})\mathbf{I}_M - g(\mathbf{x})K\mathbf{x} \quad (25)$$

This representation underlines that it is in fact a linear system that can be solved in a number of ways, but somewhat limited due to the fact that $h_s(x)$ is non-square. The law can also be represented in the implemented form, that is the form used in the MATLAB and Simulink implementations as:²

$$u = F_s \backslash (h - F_m * I_m - g * K * x)$$

where \backslash represents the matlab *mldivide*. (sec. 2.3.2)

This final formulation consists of the controller with feedback linearization implementing a pole placement controller.

5.2 Simulation

The already developed code for the system can be used to simulate both the original and, with some adaptation, the decomposed systems.³By utilizing this, the behaviour of the system in combination with the controller can be determined through simulations, which will further help in optimizing both the code and the controller.

5.2.1 Validation

The first couple of simulations were done in MATLAB in order to check the validity of the decomposed system models in comparison with the original model. These simulations include an LQR controller on a linearized version of the system in the working point $x_{eq} = [0 \ 0 \ 0.047 \ 0 \ 0 \ 0 \ 0 \ 0 \ 0 \ 0 \ 0 \ 0]^T$.

²h, F_s and F_m are equivalent to $p(x)$, $h_S(x)$ and $h_M(x)$

³Original code in "Original"-folder in https://github.com/Paalfosmo/MAGLEV_project_control

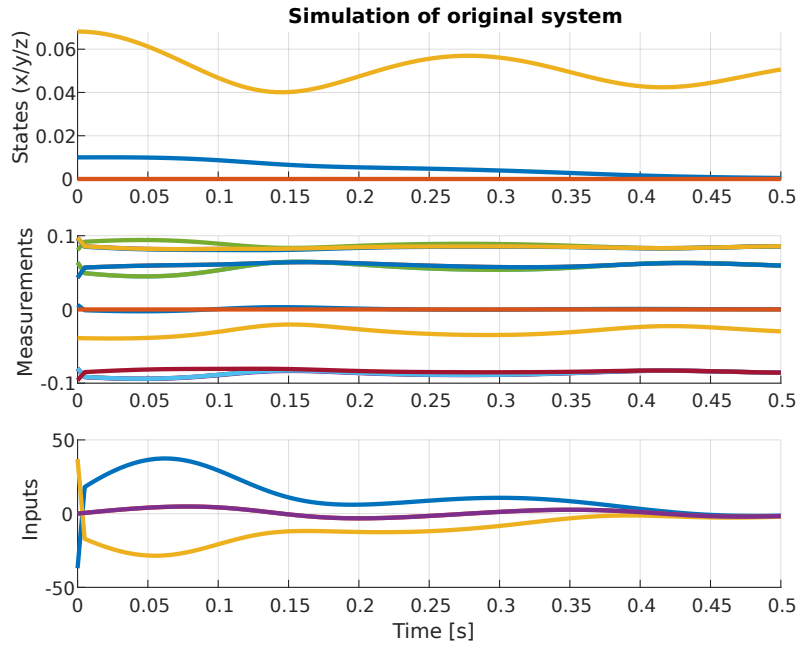


Figure 3: Simulation of the original system

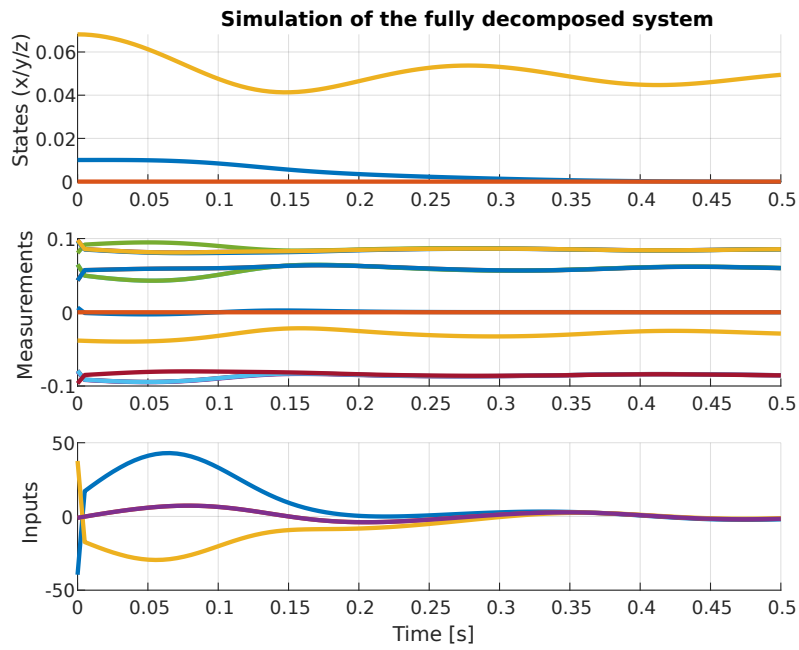


Figure 4: Simulation of the fully decomposed system (4.2.3)

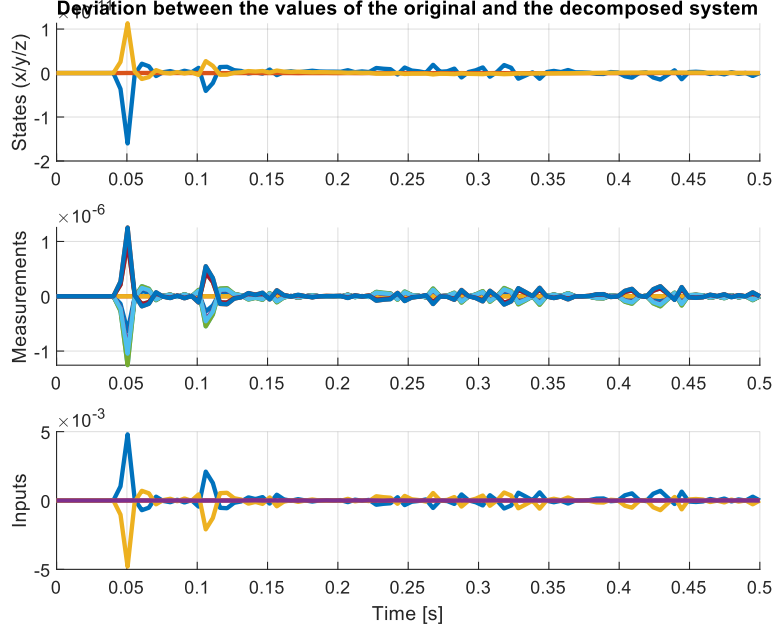


Figure 5: Deviation between the original and the decomposed system

The plots clearly indicate that the system's performance remains largely unaffected by its decomposition. The small deviations can be attributed to the numerical integration methods used in MATLAB, and are in the magnitude of $10^{-11} - 10^{-3}$. Therefore, the controller designed for the second decomposed system is applicable to the original system, suggesting that it should theoretically perform the same on the original system as it does on the decomposed.

5.2.2 Controller simulations

Building the system as a block diagram in Simulink allows the controller to be easily implemented and offers a good visualization of the dynamics at play. The following plots showcase the controller's performance in different circumstances. Common for all the simulations is the reference point, $x_{lp} = [0 \ 0 \ 0.047 \ 0 \ 0 \ 0 \ 0 \ 0 \ 0 \ 0 \ 0]^T$. For simplicity the plots only show the behaviour of x, y, z , whose control is the primary objective. The main goal of the simulations is to test the controller's ability to control the system using different bounds on the input, given that the input on the real plant must be confined to within a range in which the hardware is not destroyed.

For reference, the system was simulated using a pure pole placement controller without the feedback linearization.

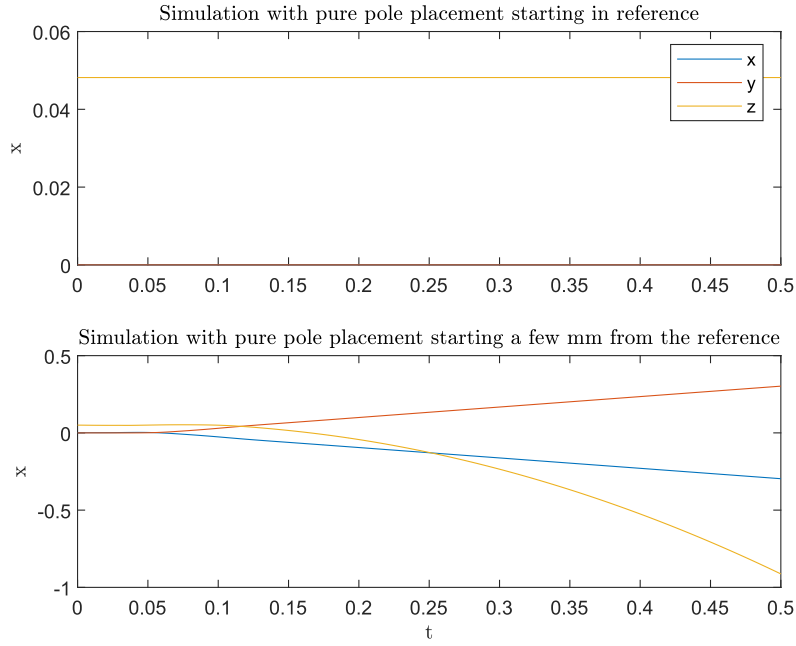


Figure 6: Simulations of the system with pure pole placement

As is evident from these two simulations, the controller fares fine when the initial conditions are identical to the reference signal. Once the initial conditions deviate slightly from the reference signal, the controller is unable to make the system converge, and stability is lost.

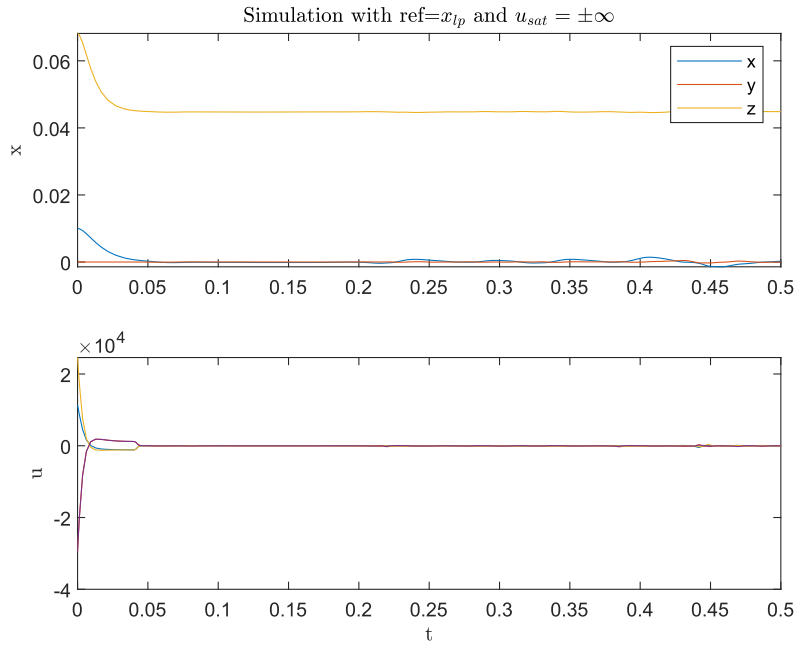


Figure 7: Simulation of the controlled system with uninhibited control inputs

Figure 7 shows the system controlled to the reference point. Notably, the utilization

of the control input is not constrained, enabling the system to rapidly converge to the specified reference point. However, this unhindered control input also results in elevated levels in the initial input.

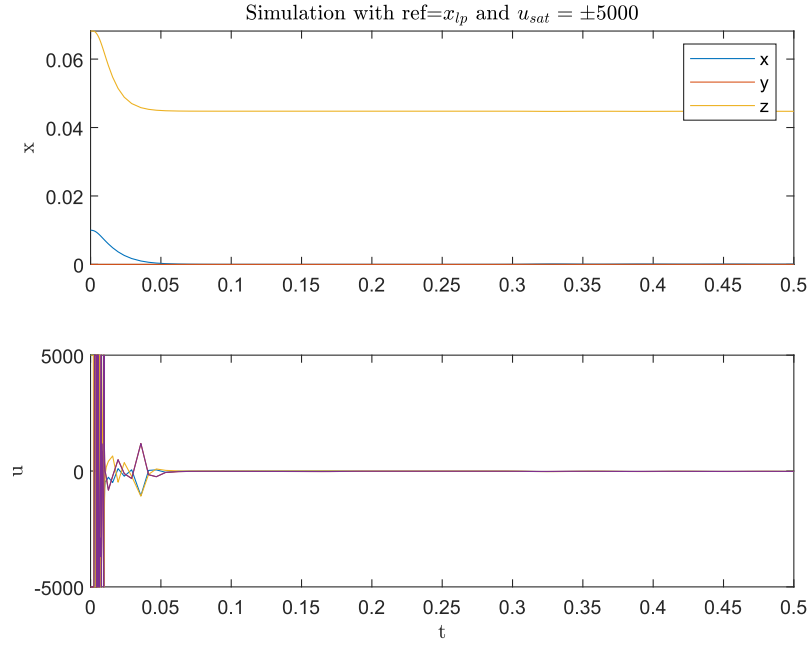


Figure 8: Simulation of the controlled system with limited control inputs

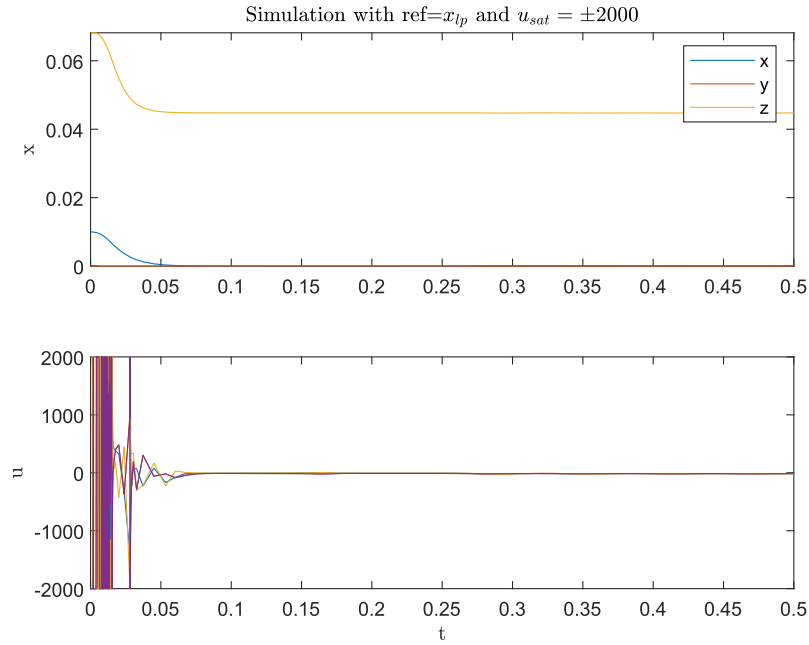


Figure 9: Simulation of the controlled system with limited control inputs

Figure 8 and 9 shows the convergence of the system when the control inputs are limited to ± 5000 and ± 2000 respectively. Clearly the limitation of the inputs im-

pacts the rate of convergence of the system as can be expected. On the other hand, it does not hinder the stability of the system in the reference point.

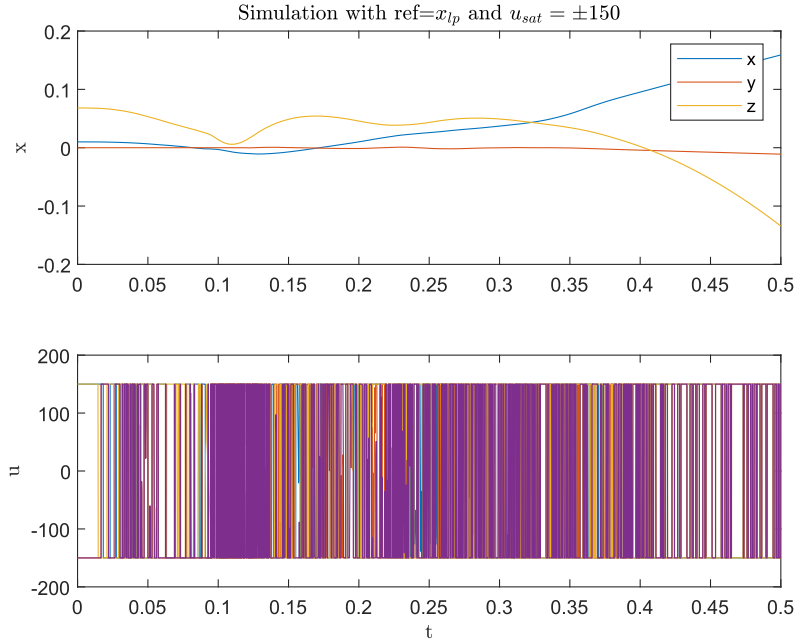


Figure 10: Simulation of the controlled system with severely limited control inputs

Figure 10 depicts the case where the inputs are confined within the range of ± 150 , exerting a noticeable influence on the stability of the system. Under these restricted input conditions, the system struggles to converge towards the reference, suggesting that the solenoids are unable to generate a force of sufficient strength to stabilize the levitating magnet.

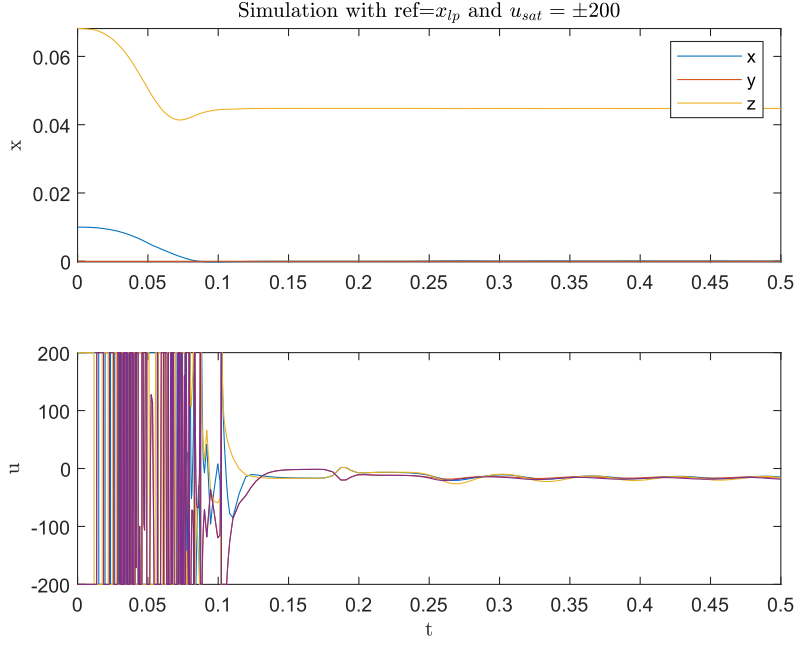


Figure 11: Simulation of the controlled system with loosened control input limits

From figure 11 it is evident that the threshold for stability of the controller lies somewhere around an input limit of ± 200 . This allows for sufficient force generation for stability whilst enabling convergence to a reference point.

In relation to how the controller performs with these limitations imposed on the input, it might also be interesting to observe how the controller reacts to steps in the reference.

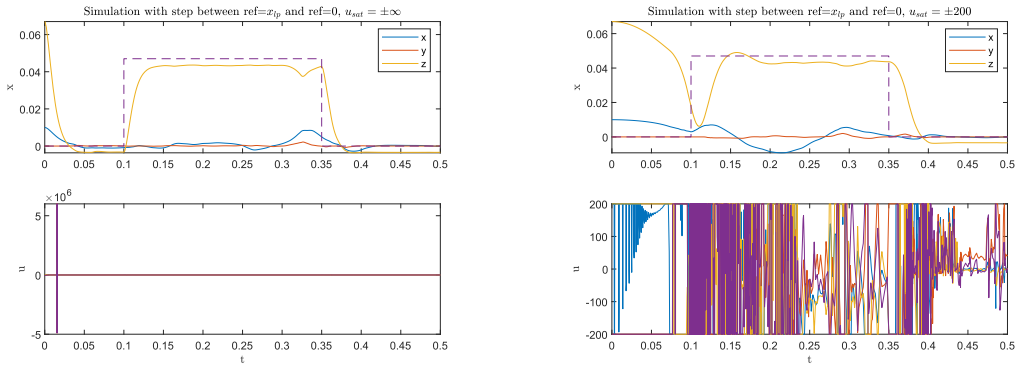


Figure 12: Simulation of the controller with step in reference without (a) and with (b) restrictions on input

From the figures above it is evident that the restrictions have some effect on the controllers performance. But it does not inhibit the controller completely, which is in line with the findings above.

5.2.3 Regions of convergence

Another way of visualizing the impact of input-restriction more intuitively is to approximate a region of convergence for the controller.

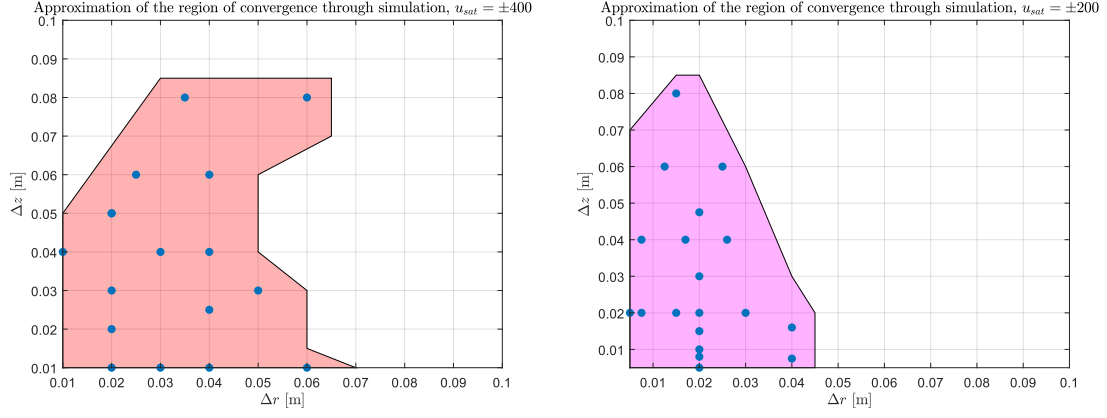


Figure 13: Approximations of the regions of convergence for two different values of the input limit

Figure 13 shows approximations of the regions of convergence in the case of $u_{sat} = 400$ and $u_{sat} = 200$. From this figure the impact of the input saturation is evident in that the region of convergence is reduced together with the input limit. The axes shows deviation from the reference point x_{lp} both in height z and radially, r . That is

$$\begin{aligned}\Delta z &= z - 0.047 \\ \Delta r &= \sqrt{x^2 + y^2}\end{aligned}$$

6 Discussion

This section will cover discussions around various issues and choices made throughout the process of developing the controller.

6.1 Choice of controller

In the development of the control scheme, it was decided early to employ a pole placement controller in the feedback linearization. This was done more out of convenience rather than optimality. Through the paper Usarman, Cahyadi, and Wahyunggoro, 2013 it was shown that this choice of controller could stabilize a maglev system in which the magnet was levitating under the actuator. Assuming that the two models were somewhat similar, it was shown that this controller also could stabilize a system where the magnet are levitating above the actuators. Other choices of control schemes, such as a plain PD-controller, might be a more optimal choice for future endeavours.

6.2 Matrix inverse

When formulating an equation for the proposed controller, some manipulation of the matrices must be done in order for the equations to be valid. The biggest challenge is inverting a non-square matrix, for which there are some methods that can be applied. Examples of this is the *matrix right inverse* or the *Moore-Penrose Inverse*, but both of these methods presupposes that the original matrix has full rank. This cannot necessarily be guaranteed for the whole domain in which the maglev should be controlled. To counter this, the MATLAB function *mldivide* was used to solve for the input which cancels the nonlinearities and controls the system to the reference. This method will yield a result for the input vector even though the matrix $h_S(\mathbf{x})$ is not full rank, although this will result in a solution which is not necessarily the minimum norm. (The MathWorks, n.d.(a))

6.3 Regions of convergence

The plots of the regions of convergence for the controller represented in the results section were generated using the simulator code. They serve to showcase the trend evident in the plots when input restrictions was applied.

Due to the nature of the magnetic fields on the maglev with the current configuration, the regions of convergence presented in this case are mere approximations. The way the magnetic fields interact with each other means that they naturally form areas where the levitating magnet is more easy to control than in others.

This means that in order to fully guarantee the region of convergence, all tests must be done on as many points along the circumference of the displacement as possible.

In the approximations presented thus far the displacements are only represented as deviations in either x or y respectively.

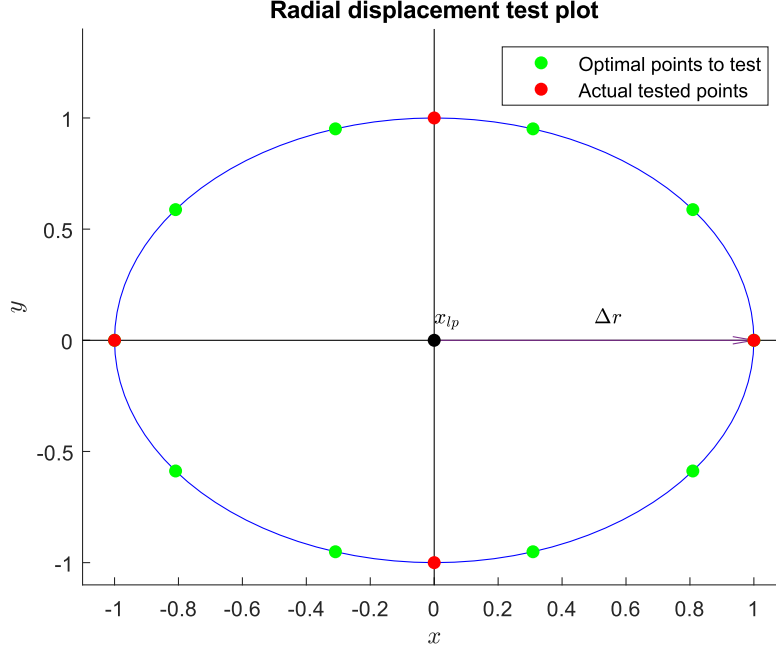


Figure 14: Example of optimal testing

Figure 14 illustrates this optimal test routine for a given Δr . In this example the optimal points to be tested for $\Delta r = 1$ together with the actual tested points are shown.

6.3.1 Stability

The reasoning above also has implications on the general stability of the physical system. Some regions far from either a permanent magnet or a solenoid will not have the necessary strength of field to accommodate levitation at all, let alone stable levitation. This is in practice not a problem, since these regions more often than not lie in the periphery of the whole platform itself.

But it does have an impact on the theoretical region in which stability can be guaranteed by the controller. The apparent solution to this is to only guarantee stability in smaller regions of the plant. For example in central parts encircled by both magnets and solenoids, which is more or less the domain the controller should be able to stabilize anyways.

6.4 Limitation of the input

During the controller tests, it became evident that addressing input saturation was essential. Consequently, a primary objective of the report became to assess whether

the impact on the stability of the controller could influence the feasibility of implementing it on the physical system.

The limitations on the input was simulated by using a *saturation*-block in Simulink. This block allows for upper and lower bounds on the signal to be applied directly, and is the easiest solution when it comes to limiting a signal. This is by far the optimal solution to this problem. In a case where the control law v contains an integrator, this might lead to *wind-up* and further compromise the controllers ability to react to changes in the reference. (Andresen, Balchen, and Foss, 2016)

In the simulations this is not a problem, and since the chosen controller lacks an integrator it had no further implications with regards to controller performance. When the time comes to implement the controller on the physical system, one might want to solve this differently. An example could be to model the restrictions on the input in the system dynamics in some way, but the feasibility of this is also dependent on the complexity it will add in an already complicated system.

6.5 System identification

In this implementation of the feedback linearizing controller, the simulations were conducted using the full state-space directly with exact and noiseless state measurements. This will not be the case in practice. Generally, the position of the levitating magnet must be read from the measurements offered by the hall-effect sensors which only measures the magnetic fields. This means that the position and state of the levitating magnet is not readily available per se, but can be estimated using an estimator or observer.

When the controller is implemented on the physical system, this is where the main challenge lies. Some modifications must be made in order to accommodate the fact that it will only be able to react to estimations of the real states. Two of the states are also uncontrollable with the current configuration, which will also need to be reflected in the controller's formulation. In spite of this, the controller developed and the simulations done in this report will serve as a *proof of concept* with regards to implementation on the physical plant.

7 Further work

This section will describe the longer term goal of the controller in the project, as well as detail what tasks lie ahead in the development of the system with regard to the controller.

7.1 Implementation

The obvious long-term goal is the successful implementation of the controller on the physical maglev system. The first step is to adapt the controller such that it can work alongside an observer and make calculations based on this whilst remaining stable. This entails making changes to the state space and modifying the controller accordingly, both to reflect the uncontrollability of some of the states and to accommodate possible deviations in the delivered estimates. Other challenges and tasks include the input saturation problem as described earlier and how to deal with it, together with the computational complexity of the current solution and how to optimize the code as much as possible.

7.2 Stability

Among the practical issues that might be faced in relation to the physical implementation revolves around stability. More specifically it might be interesting to produce an actual plot of the region of convergence on the physical system and compare it to the approximation. This will provide a good starting point for closer analysis of the controller's stability and the system as a whole.

As presented in this report, the limitation on the input signal has a big impact on the stability of the controller. It is evident that the scenario with input limitations is a highly realistic one on the physical system, and therefore it is reasonable to consider whether the limitation is so low on the physical system that it will render the controller unstable. This hinges on the limitations on the electromagnets, and analysing where this limit lies will be very important to realize the controller.

7.3 Other control approaches

Other ways of controlling the system might also be interesting to try. Whether they are advanced or not. The method used in this report, pole placement, is most likely not the optimal controller to choose in the feedback linearization-scheme. Other controllers might be better suited to the system, for example just a plain PID- or PD-controller, preferably with anti-windup if input limitation is used. Other advanced methods might also be up for consideration outside of feedback linearization.

8 Conclusion

A controller for the maglev system based on feedback linearization is feasible. The feedback linearization lays the foundation for other control schemes to function on this nonlinear system, and through testing and simulation a feedback linearizing controller is in theory possible to deduce. By manipulating the system formulation it is quite possible to find the exact input signal which realizes the feedback linearization. The stability of the controller is dependent on the circumstances in which it is implemented, one of the main points being restrictions on the usage of the input.

Restrictions on the inputs have been shown to have a impact on the controllers ability to control the system, and also on the region of convergence for the controller. To remedy this other linear control methods might be considered implemented on top of the feedback linearization. It is also important that the actual limitations on the physical system are so low that the controller cannot function in practice.

In conclusion, should the physical limitations, such as the electromagnets, allow for it, a controller based on feedback linearization should be able to control the system and provide the desired stability.

References

- Andresen, T., J. G. Balchen, and B. A. Foss (2016). *Reguleringsteknikk*. no. Institutt for teknisk kybernetikk, NTNU.
- Coey, J. M. D. (2010). *Magnetism and magnetic materials*. en. Cambridge University Press.
- Engmark, H. A. and K. T. Hoang (2023). “Modeling and Control of a Magnetic Levitation Platform”. In: *IFAC-PapersOnLine* 56.2. 22nd IFAC World Congress, pp. 7276–7281. DOI: <https://doi.org/10.1016/j.ifacol.2023.10.338>. URL: <https://www.sciencedirect.com/science/article/pii/S240589632300705X>.
- González, M. A. and D. E. Cárdenas (2021). “Analytical Expressions for the Magnetic Field Generated by a Circular Arc Filament Carrying a Direct Current”. In: *IEEE Access* 9, pp. 7483–7495. DOI: 10.1109/ACCESS.2020.3044871.
- Grant, I. S. (1990). *Electromagnetism*. en. Wiley.
- Khalil, H. K. (2002). *Nonlinear Systems*. en. Prentice Hall.
- Lipschutz, S., M. R. Spiegel, and D. Spellman (2009). *Schaum’s Outline of Vector Analysis, 2ed.* en. McGraw Hill Professional.
- Ravaud, R. et al. (2010). “Cylindrical Magnets and Coils: Fields, Forces, and Inductances”. In: *IEEE Transactions on Magnetics* 46.9, pp. 3585–3590. DOI: 10.1109/TMAG.2010.2049026.
- Sadiku, M. N. O. (2001). *Elements of Electromagnetics*. en. Oxford University Press, USA.
- Slotine, J. E. and W. Li (1991). *Applied Nonlinear Control*. Prentice Hall, Inc.
- The MathWorks, I. (n.d.[a]). *Solve systems of linear equations $Ax = B$ for x - MATLAB mldivide*. URL: <https://se.mathworks.com/help/matlab/ref/mldivide.html> (Accessed on 23/11/2023).
- (n.d.[b]). *Trapezoidal numerical integration - MATLAB trapz*. URL: <https://se.mathworks.com/help/matlab/ref/trapz.html> (Accessed on 23/11/2023).
- Uswarman, R., A. I. Cahyadi, and O. Wahyunggoro (2013). “Control of a magnetic levitation system using feedback linearization”. In: *2013 International Conference on Computer, Control, Informatics and Its Applications (IC3INA)*, pp. 95–98. DOI: 10.1109/IC3INA.2013.6819156.